Journal of the European Ceramic Society 22 (2002) 2489–2494

www.elsevier.com/locate/jeurceramsoc

High performance porous silicon nitrides

Yoshiaki Inagaki[a], Naoki Kondo[b], Tatsuki Ohji[b,*]

[a]*Synergy Ceramics Laboratory, Fine Ceramics Research Association, Nagoya 463-8687, Japan*
[b]*Synergy Materials Research Center, National Institute of Advanced Industrial Science and Technology, Nagoya 463-8687, Japan*

Received 10 October 2001; accepted 14 April 2002

Abstract

In structural materials, pores are generally believed to deteriorate the mechanical reliability. This study, however, demonstrates pores can cause improved or unique performance when the porous microstructure is carefully controlled. The first example is a silicon nitride of 14% porosity fabricated by tape-castng whiskers. This material, where the characteristic fibrous grains were aligned uniaxially, shows a high fracture strength in excess of 1 GPa as well as high damage tolerance. The fracture energy obtained by a chevron-noteched beam technique was about seven times larger than that of dense silicon nitride, which was primarily attributable to grain ''pull-out'' mechanism enhanced by the pores. The other example was a silicon nitride of 24% porosity, fabricated by sinter forging technique which exhibited excellent strain tolerance.

Keywords: Fracture; Mechanical properties; Porosity; Si_3N_4; Tape casting

1. Introduction

A number of approaches have been applied to improve the fracture toughness of ceramics. As for silicon nitride, there have been many studies about toughening by controlling microstructures, such as grain size and morphology, grain alignment, and boundary chemistry to enhance a variety of crack wake toughening mechanisms including grain bridging and grain pull-out.[1–7] Aligning fibrous silicon nitride grains using a tape-casting technique with seed particles, Hirao et al.[8] obtained high fracture toughness, ~11 MPa $m^{1/2}$ as well as high fracture strength, ~1100 MPa when a stress was applied parallel to, or a crack extended normal to, the grain alignment. In this case, a greater number of fibrous grains are involved with the crack wake toughening mechanisms, and then the toughness can rise steeply in a very short crack extension.[9] Moreover, Kondo et al.[10] succeeded in better alignment of fibrous grains through a superplastic deformation in plane-strain compression, realizing higher fracture toughness, ~13 MPa $m^{1/2}$, and higher fracture strength, ~1650 MPa.

In brittle ceramic materials, strains which are undesirably generated cannot be relaxed by plastic deformation. This often leads to the abrupt fracture even with a small strain, particularly for high-elastic-modulus materials. Then, if the elastic modulus can be lowered while retaining strength, strain-to-failure can become larger, ensuring the structural reliability. Based on such a concept, Shigegaki et al.[11] developed a porous silicon nitride with a porosity of 14.4% by tape-casting method from fibrous silicon nitride grains, where the grains were uniaxially aligned; this material has a high fracture strength, ~1080 MPa, as well as a low elastic modulus, 246 GPa. Since the pores exist around the aligned fibrous grains, enhanced operations of the grain bridging and pull-out can be anticipated when the crack propagates perpendicularly to the direction of grain alignment. Furthermore, the presence of pores surrounding the silicon nitride grains causes cracks to tilt or twist, namely crack deflections.[12,13] Keeping this in mind, this study is aimed at investigating fracture resistance behaviors of this porous silicon nitride.

In addition we also intend to apply the sinter-forging technique for fabricating the porous silicon nitride with aligned fibrous grains. Initial silicon nitride powders, which mainly consist of α-phase, have an equiaxed shape, but elongate through phase transformation to β-phase and Ostwald ripening during soaking at elevated

* Corresponding author. Tel.: +81-52-739-0155; fax: +81-52-739-0136.
E-mail address: t-ohji@aist.go.jp (T. Ohji).

0955-2219/02/$ - see front matter
PII: S0955-2219(02)00107-3

temperatures. In this process, forging pressure is applied after the grain elongation until reaching a desired porosity, which will lead to a porous microstructure with aligned silicon nitride fibrous grains. The performance of the obtained porous silicon nitride is also demonstrated in this paper.

2. Experimental procedures

The fabrication of the porous silicon nitride through tape casting (hereafter designated PSN-TC) has been reported elsewhere,[11,14] but is briefly described here. For starting powders, β-silicon nitride whiskers were mixed with 5 wt.% yttria and 2 wt.% alumina. The green sheets which were formed by tape casting were stacked and bonded under pressure. Sintering was performed at 1850 °C under a nitrogen pressure of 1 MPa. Fig. 1 shows the microstructure of the material; the fibrous grains of silicon nitride are well aligned toward the casting direction, and the pores exist among the grains. For comparison, the fracture resistance behavior of a reference material (hereafter RSN), which was fabricated using α-silicon nitride powders with sintering additives 5 wt.% yttria and 2 wt.% alumina,[11] was characterized by the same testing procedures. Flexural test specimens, whose nominal dimensions are 4.0 mm in height, 3.0 mm in width, and 35 mm in length, were cut from the sintered billets so that the tensile axis and tensile surface were parallel to the casting direction and the stacking plane, respectively. Details of the employed chevron-notched specimen geometry and testing procedures were the same as those that had been used for a previous study.[15] The shape of the ligament was a regular triangle with an edge length of 3 mm, and the initial crack length, a_0, was 1.4 mm. The width of the chevron-notch was 100 μm, and the fracture testing was carried out at room temperature when three-point bending with a lower span of 30 mm at a cross-head speed of 0.01 mm/min. A bending fixture of silicon carbide was used to realize high rigidity of the testing system, which is needed for stable crack growth. The true load–displacement (*L-D*) curve was determined by subtracting the compliance of the testing machine and the fixture, which was obtained in advance by an independent calibration, from the experimentally observed curve.

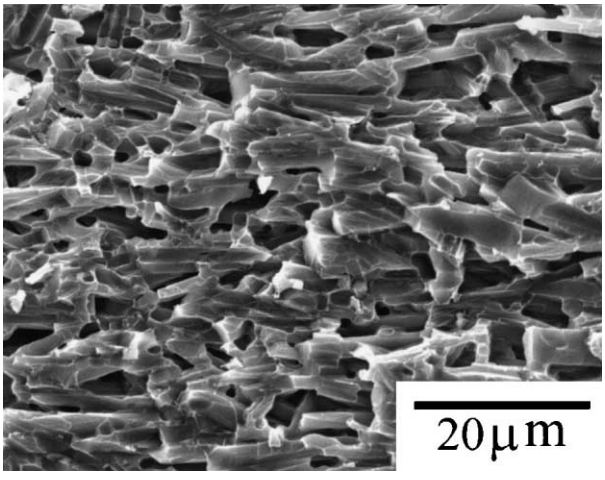

Fig. 1. SEM micrograph of polished and plasma-etched top surface of the PSN-TC.

For producing the porous silicon nitride through sinter-forging (hereafter desiganated PSN-SF), α-silicon nitride powder (Ube, E10) was used as the starting powder. It was mixed with 5 wt.% Y_2O_3 (Shinetsu, UF) as the sintering additive, and was ball-milled for 50 h in methanol using silicon nitride balls. The powder was dried, sieved and compacted with a uniaxial pressure of 2.5 MPa in a graphite die with a base of 45 × 45 mm. Partial sinter-forging was conducted using a hot-press furnace. The atmosphere inside the furnace, nitrogen gas (99.99%) under 0.1 MPa pressure, was maintained throughout the process. The graphite die was heated to 1850 °C at a rate of 10 °C·min^{-1}. After soaking for 30 min, uniaxial mechanical pressure of 6000 kg (approximately 30 MPa) was applied for 150 min (therefore, total soaking time at 1850 °C was 180 min). Piston transfer was restricted to control the density of the sintered specimen. After the procedure, the die was cooled at a rate of 10 °C min^{-1} to <1000 °C. Specimens of 3 × 4 × 40 mm for measuring the bending strength were cut from the partially sinter-forged body so that the stress face was perpendicular to the pressing direction. All faces were finished lengthwise by a 400 grid diamond wheel, and the edges were chamfered using an 800 grid diamond whetstone. Three-point bending strength was measured with a span of 30 mm with a cross-head speed of 0.5 mm/min at room temperature.

Density of the specimen was measured by the Archimedes method. Elastic modulus was measured by the pulse echo method. Microstructure of the specimen was observed on the fractured surfaces by scanning electron microscopy (SEM). X-ray diffraction analysis was conducted to examine the phases in the specimen, as well as to examine the orientation of silicon nitride grains. These characterizations were conducted for the top and side planes (planes normal and parallel to the pressing direction, respectively) of the fabricated specimen.

3. Results and discussion

3.1. Porous silicon nitride through tape casting

Five specimens were used for each characterization, and continuously stable crack growth up to the point of fracture was obtained for a few specimens of both the PSN-TC and RSN with sufficient reproducibility of the *L–D* curves; the other measurements resulted in undesirable

catastrophic failure during testing. Successful examples of the *L–D* curves for the two materials are shown in Fig. 2.

While the RSN showed a smooth *L–D* curve which is normally observed for chevron-notched beam tests of monolithic ceramic materials, the PSN-TC demonstrated serrations in the almost entire region, suggesting repetition of crack initiations and arrests. The curve of the PSN-TC in Fig. 2 is that after leveling the serration. The effective fracture energy, γ_{eff}, is defined as follows:

$$\gamma_{eff} = W_{WOF}/2A \quad (1)$$

where W_{WOF} is the energy under *L–D* curve, and A is the area of the specimen web portion. By substituting W_{WOF} calculated from Fig. 2 into Eq. (1), one can obtain 492.7 J/m^2 and 70.2 J/m^2 as γ_{eff} of the PSN-TC and RSN, respectively. Note that γ_{eff} of the PSN-TC is about seven times larger than that of the RSN. It is also enormously high compared with those of other toughened silicon nitrides, such as 96 J/m^2 of a silicon-carbide-whisker-reinforced dense silicon nitride,[15] and 246 J/m^2 of a highly anisotropic silicon nitride produced by superplastic deformation.[16] (These values were measured using exactly the same CNB test techniques.)

This large fracture energy is attributable to the crack wake toughening mechanisms of silicon nitride[17–19] which are classified into two categories: (1) bridging of the crack by unbroken fibrous reinforcing grains that is partially debonded from the matrix (grain bridging), (2) frictional pull-out of fibrous grains (grain pull-out). For these mechanisms to operate, debonding of the interface between the matrix and the fibrous grains is a necessary condition. In dense silicon nitrides where interfaces are relatively strong, such debonding is restricted and then the toughening mechanisms are not fully operated. In the PSN-TC, however, the pores existing around the grains would enhance the debonding, leading to the activated crack-wake toughening mechanisms. Fig. 3 shows the SEM image of the fracture surface of the test specimen where the fibrous grains have been pulled out, supporting this speculation.

The fracture toughness is defined as follows:

$$K_{IC} = (2E'\gamma_{eff})^{1/2} \quad (2)$$

where E' is the Young's modulus for plane strain condition, which is given by $E' = E/(1-\nu^2)$ with ν being the Poisson's ratio. Substituting 246 GPa and 325 GPa as the Young's moduli of the PSN-TC and RSN, respectively[11] and 0.25 as the Poisson's ratio into Eq. (2), K_{IC} becomes 16.1 MPa m$^{1/2}$ for the PSN-TC and 7.0 MPa m$^{1/2}$ for the RSN.

Moreover, a stress intensity factor, K_I, can be estimated from the CNB tests using Bluhm's synthesized numerical slice model, as follows;[20,21]

$$K_I = [(E'/2)(dx/dA)]^{1/2}P \quad (3)$$

where x is the compliance, A is the crack area, and P is the load. The crack length corresponding to a load can also be calculated from the change in specimen compliance, and the variation of fracture resistance with crack extension (namely *R*-curve) thus can be obtained. It should be noted, however, that the bridging traction in the crack wake as shown later would influence the specimen compliance, raising some concern about the accuracy of this technique, and that only crude estimation of *R*-curve was possible. The fracture resistance curves of the PSN-TC and RSN are shown in Fig. 4, where a and W represent the crack length and the height of a specimen, respectively. The PSN-TC *R*-curve reaches higher values than does that of the RSN. The resistance increases almost lineally with the crack

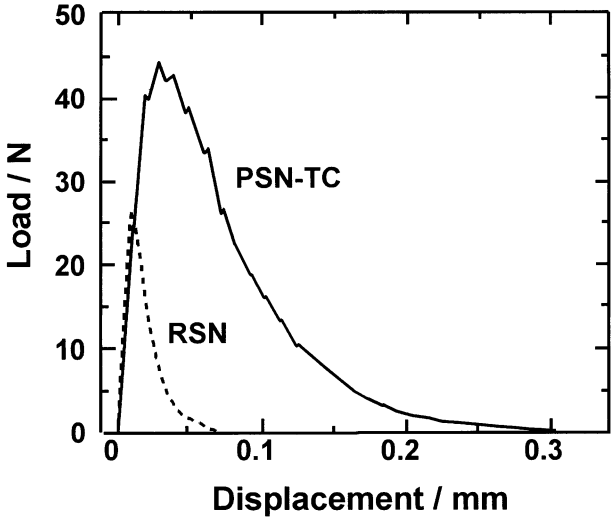

Fig. 2. Load-deflection diagrams of the chevron-notched bend tests for the PSN-TC and RSN.

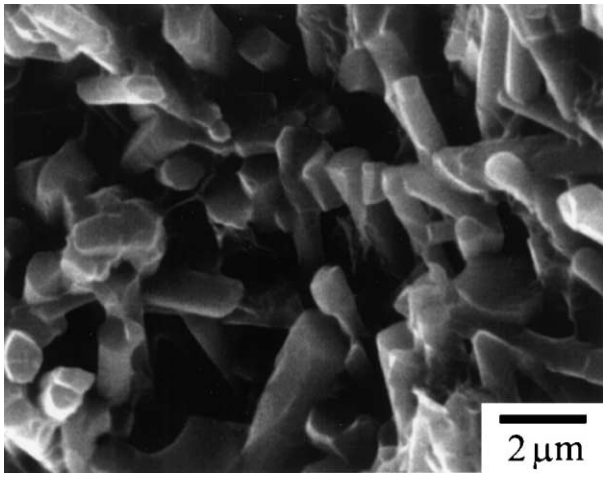

Fig. 3. SEM micrograph of the ligament area of fracture surface for the PSN-TC.

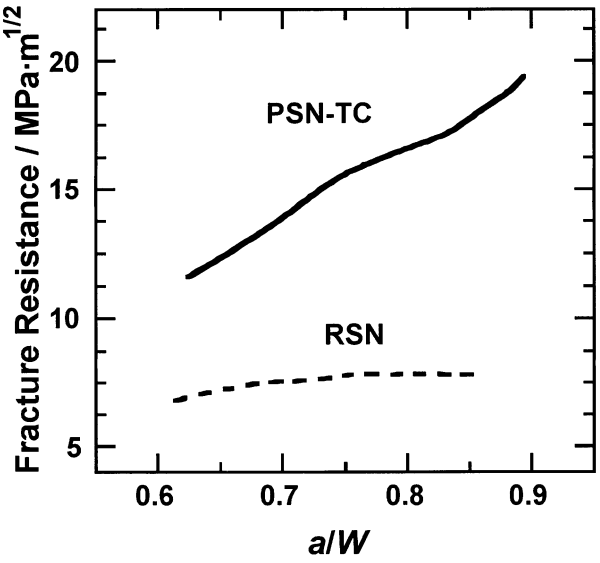

Fig. 4. *R*-curve behaviors in the chevron-notched bend tests for the PSN-TC and RSN.

extension and reaches a very high value, about 20 MPa $m^{1/2}$, around the a/W of 0.9.

This rising *R*-curve behaviors is also attributable to the same crack wake toughening as mentioned above. It has been known that a steep rise of fracture resistance in a short crack extension (typically several microns to several ten microns) is primarily attributable to grain bridging, while grain pull-out gives rise to an increased resistance after a long crack extension (typically several hundred microns).[9,22] The *R*-curve of the PSN-TC in Fig. 4 is very likely caused by the latter. This speculation is also supported from Fig. 3 which shows the fibrous grains have been pulled out.

As stated in the introduction, the PSN-TC has a fracture strength, ~1080 MPa, which is very high for a silicon nitride with a porosity of 14.4%. It has been known, however, that an increased resistance after a long crack extension such as the *R*-curve of the PSN-TC contributes little to an increase of fracture strength.[9] Thus, it can be presumed that the toughening associated with a very short crack extension such as the grain bridging and crack deflection, is active in the present material.

3.2. Porous silicon nitride through sinter-forging

For the PSN-SF, the sinter-forging was conducted so that the porosity became around 25%. The relative density of the obtained density was 76.0%. Microstructure of the specimen is shown in Fig. 5. It can be known that the fibrous grains, whose size is substantially small compared to that of the PSN-TC, tend to align in horizontal direction. The microstructure also shows protruding fibrous grains as well as holes or hollows as noted by arrows. The X-ray diffraction analysis revealed the anisotropy more clearly as shown in Fig. 6. These patterns were taken from the top and side planes, respectively. The fabricated specimen was found to consist of β-silicon nitride grains (ASTM card 33–1160). The (210) peak was remarkably higher in the top plane, and lower in the side plane, than the (101) peak. This means the prismatic plane of the silicon nitride grains tended to be aligned perpendicularly to the pressing direction, since (101) and (210) peaks should have approximately the same heights in the case of isotropic silicon nitride. Therefore, the porous microstructure with two-dimensionally oriented β-silicon nitride grains were successfully formed by the partial sinter-forging technique. In fabricating the PSN-SF, mechanical pressure was applied after grain elongation. The relative density of the green compact in the graphite die was roughly

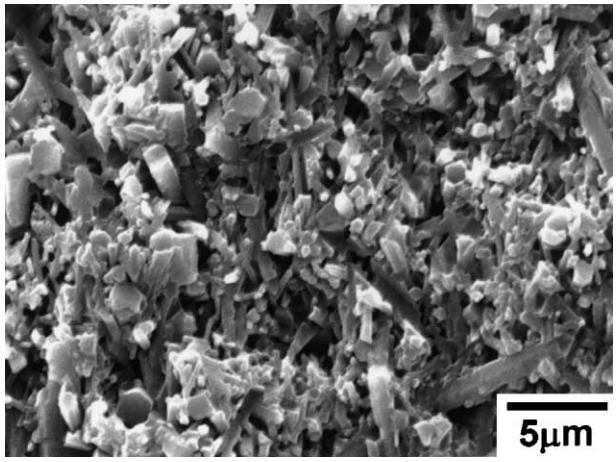

Fig. 5. Microstructure of the PSN-SF. The micrograph was taken from the fractured side surface. Some of the typical protruding fibrous grains are noted by arrows.

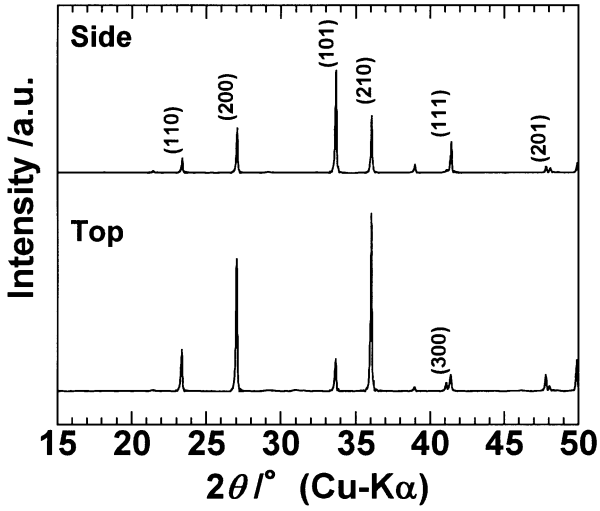

Fig. 6. X-ray diffraction analysis of the PSN-SF. These patterns were taken from the top and side planes, respectively.

estimated as 45–50%, therefore, height reduction of 25–30% could be applied by the partial sinter-forging, resulting in the anisotropic microstructure. From the previous studies,[22,23] the larger the silicon nitride deformed, the higher the anisotropy would be. Therefore, we should obtain a material with lower porosity and higher anisotropy, or with higher porosity and lower anisotropy, by choosing the sinter-forging condition. The elastic modulus and strength of the fabricated specimen are summarized in Table 1. The modulus was 150 and 183 GPa, for the top and side planes, respectively. Elastic anisotropy of β-silicon nitride grain was measured by Hay et al.[25] and Vogelgesang et al.,[26] i.e. the elastic is 450–540 GPa in the direction parallel to the *c*-axis, and is 280–310 GPa perpendicular to it. Thus this elastic anisotropy should originate from the anisotropic microstructure.

The specimen exhibited relatively high bending strength of 778 MPa for the large porosity of 24%. The high strength combined with the low elastic molulus leads to large fracture strain, or high strain tolerance of the material. This high strength for the porous material is very likely due to the grain alignment effects. Toughening of silicon nitride generally arises by crack wake toughening mechanisms including bridging of the crack by unbroken fibrous grains.[17] In silicon nitride with aligned fibrous grains, fracture resistance is steeply raised in short crack propagation because of effective operation of the grain bridging, leading to the improved strength.[9] Another possible reason for the high strength is the decreased flaw size by sinter-forging. Even if the large defects exist in the green compact, their sizes can be substantially reduced by the forging,[24,27] since the green compact shrinks in the pressing direction.

Table 1
Characteristics of the PSN-SF[a]

Relative density (%)	Open pore (%)	Closed pore (%)	Elastic modulus (GPa)	Strength (MPa)
76	21.8	2.2	150 (top) 183 (side)	778±17

[a] Five specimens were used for measurement of bending strength, and it is shown as a mean value with the standard deviation.

3.3. Comparison of properties of the porous and dense silicon nitrides

Fig. 7 compares fractrue energy, strength, fracture strain and lightweighness of the RSN, ITSN, PSN-TC, and PSN-SF. The ITSN is a dense silicon nitride, which is in-situ toughened by coarse microstructure.[2] For all the materials, the fracture energy was measured by the above described CNB test technique. The fracture strain is given by dividing the strength by the elastic modulus, and the lightweight is expressed by a reciprocal of the specific gravity. When applying a stress parallel to the grain alignment, the porous materials show almost equivalent strength to that of the dense materials. As for the fracture energy or damage tolerance, however, the porous materials are even more advantageous than the dense materials. This is typical in the PSN-TC where coarse fibrous grains are aligned. On the other hand, as seen in the PSN-SF (fine fibrous grain alignment), it is possible to introduce pores with little sacrificing of the strength. In this case, the elastic modulus decreases by almost half at 24% porosity and the fracture strain or strain tolerance becomes great substantially. Increased porosity also further improves the lightness that is an intrinsic characteristic of ceramic materials; the 24%

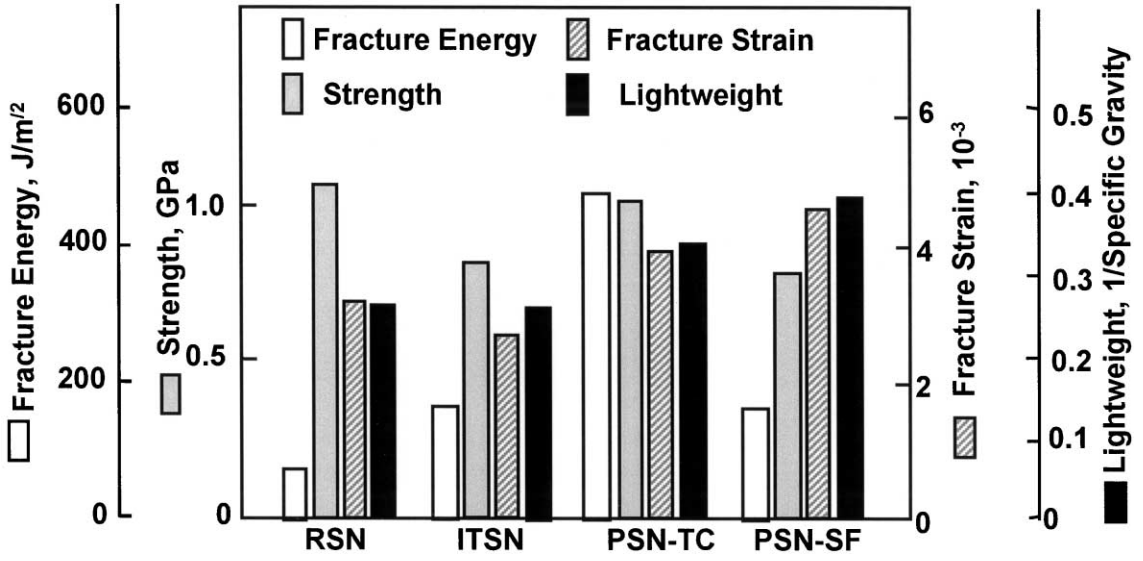

Fig. 7. Comparison of fractrue energy, strength, fracture strain and lightweight of the RSN, ITSN, PSN-TC, and PSN-SF. The ITSN is an in-situ toughened dense silicon nitride. Porosity of the PSN-TC and PSN-SF is 14 and 24%, respectively.

porosity leads to the 24% weight reduction. Consequently, the existence of pores does not necessarily lead to degradation of properties in ceramics. By controlling the size, shape and alignment of pores as well as matrix grains, excellent or unique performance can be drawn out.

4. Summary

This study demonstrated that the pores can cause improved or unique performance of porous materials whenever the porous microstructure is carefully controlled. The first example was a silicon nitride of 14% porosity where the characteristic elongated grains were aligned uni-axially (anisotropic microstructure). This material showed a high fracture strength in excess of 1 GPa as well as high damage tolerance; the fracture energy determined by a chevron-notched beam technique was seven times larger than that of dense silicon nitride. This was primarily attributable to grain "pull-out" enhanced by the pores presence. Furthermore, the porosity is useful in reducing weight of the component and increasing the strain tolerance and the thermal shock resistance. The second example was silicon nitride of 24% porosity, which was fabricated by sinter forging technique. It exhibited excellent strain tolerance as well as one-fourth weight reduction. Moreover, the low elasticity modulus combined to a high strength also leads to excellent thermal shock fracture resistance.

Acknowledgements

This work has been promoted by AIST, MITI, Japan as a part of the Synergy Ceramics Project under the Industrial Science and Technology Frontier (ISTF) Program. Under this program, part of the work has been supported by NEDO. The authors are members of the Joint Research Consortium of Synergy Ceramics.

References

1. Tani, E., Umebayashi, S., Kishi, K., Kobayashi, K. and Nishijima, M., Gas-pressure sintering of Si_3N_4 with concurrent addition of Al_2O_3 and 5 wt.% rare earth oxide. *Am. Ceram. Soc. Bull.*, 1995, **65**, 1311–1315.
2. Kawashima, T., Okamoto, H., Yamamoto, H. and Kitamura, A., Grain size dependence of the fracture toughness of silicon nitride. *J. Ceram. Soc. Jpn.*, 1990, **98**, 235–242 (in Japanese.).
3. Mitomo, M. and Uenosono, S., Microstructural development during gas-pressure sintering of a-silicon nitride. *J. Am. Ceram. Soc.*, 1992, **75**, 103–108.
4. Goto, Y. and Tsuge, A., Mechanical properties of unidirectionally oriented SiC-whisker reinforced Si_3N_4 fabricated by extrusion and hot-pressing. *J. Am. Ceram. Soc.*, 1993, **76**, 1420–1424.
5. Hirosaki, N., Akimune, Y. and Mitomo, M., Effect of grain growth of β-silicon nitride on strength, meibull modulus and fracture toughness. *J. Am. Ceram. Soc.*, 1995, **78**, 1687–1690.
6. Becher, P. F., Lin, H. T., Hwang, S. L., Hoffmann, M. J. and Chen, I.-W., The influence of microstructure on the mechanical behavior of silicon nitride ceramics. In *Silicon Nitride Ceramics*, ed. I.-W. Chen, P. F. Becher, M. Mitomo, G. Petzow and T. S. Yen. Material Research Society, Pittsburgh, PA, 1993, pp. 147–158.
7. Hirao, K., Nagaoka, T., Brito, M. E. and Kanzaki, S., Microstructure control of silicon nitride by seeding with rodlike b-silicon nitride particles. *J. Am. Ceram. Soc.*, 1995, **78**, 1857–1862.
8. Hirao, K., Ohashi, M., Brito, M. E. and Kanzaki, S., Processing strategy for producing highly anisotropic silicon nitride. *J. Am. Ceram. Soc.*, 1995, **78**, 1687–1690.
9. Ohji, T., Hirao, K. and Kanzaki, S., Fracture resistance behavior of highly anisotropic silicon nitride. *J. Am. Ceram. Soc.*, 1995, **78**, 3125–3128.
10. Kondo, N., Suzuki, Y. and Ohji, T., Superplastic sinter-forging of silicon nitride with anisotropic microstructure formation. *J. Am. Ceram. Soc.*, 1999, **82**, 1067–1069.
11. Shigegaki, Y., Brito, M. E., Hirao, K., Toriyama, M. and Kanzaki, S., Strain tolerant porous silicon nitride. *J. Am. Ceram. Soc.*, 1997, **80**, 495–498.
12. Faber, K. T. and Evans, A. G., Crack deflection processes I. Theory. *Acta. Metall.*, 1983, **31**, 565–576.
13. Faber, K. T. and Evans, A. G., Crack deflection processes II. Experimental. *Acta. Metall.*, 1983, **31**, 577–584.
14. Shigegaki, Y., Brito, M. E., Hirao, K., Toriyama, M. and Kanzaki, S., Processing of a novel multilayered silicon nitride. *J. Am. Ceram. Soc.*, 1996, **79**, 2197–2200.
15. Ohji, T., Goto, Y. and Tsuge, A., High temperature toughness and tensile strength of whisker reinforced silicon nitride. *J. Am. Ceram. Soc.*, 1991, **74**, 739–745.
16. Kondo, N., Inagaki, Y., Suzuki, Y. and Ohji, T., High-temperature fracture energy of superplastically forged silicon nitride. *J. Am. Ceram. Soc.*, 2001, **84**, 1791–1796.
17. Becher, P. F., Hwang, S. L., Lin, H. T. and Tiegs, T. N., Microstructural contribution to the fracture resistance of silicon nitride ceramics. In *Tailoring of Mechanical Properties of Si3N4 Ceramics*, ed. M. J. Hoffmann and G. Petzow. Kluwer Academic Publishers, the Netherlands, 1994, pp. 87–100.
18. Becher, P. F., Microstructural design of toughened ceramics. *J. Am. Ceram. Soc.*, 1991, **74**, 255–269.
19. Steinbrech, R. W., Toughening mechanisms for ceramic materials. *J. Eur. Ceram. Soc.*, 1992, **10**, 131–142.
20. Bluhm, J. I., Slice synthesis of a three dimensional work of fracture specimen. *Eng. Fract. Mech.*, 1975, **7**, 593–604.
21. Sakai, M. and Yamasaki, K., Numerical fracture analysis of chevron-notched specimens: I, shear correction factor, k. *J. Am. Ceram. Soc.*, 1983, **66**, 371–375.
22. Ohji, T., Kondo, N., Suzuki, Y. and Hirao, K., Grain bridging of highly anisotropic silicon nitride. *Mat. Lett.*, 1999, **40**, 5–10.
23. Kondo, N., Sato, E. and Wakai, F., Geometrical microstructural development in superplastic silicon nitride with rod-shaped grains. *J. Am. Ceram. Soc.*, 1998, **81**, 3221–3227.
24. Kondo, N., Ohji, T. and Wakai, F., Strengthening and toughning of silicon nitride by superplastic deformation. *J. Am. Ceram. Soc.*, 1998, **81**, 713–716.
25. Hay, J. C., Sun, E. Y., Pharr, G. M., Becher, P. F. and Alexander, K. B., Elastic anisotoropy of β-silicon nitride whiskers. *J. Am. Ceram. Soc.*, 1998, **81**, 2661–2669.
26. Vogelgesang, R., Grimsditch, M. and Wallace, J. S., The elastic constants of single crystal b-Si_3N_4. *Appl. Phys. Lett.*, 2000, **76**, 982–984.
27. Imuta, M., Gotoh, J., Nakayama, H. and Wakai, F., Superplasiticy and compressive forming of Y-TZP. *Trans. Mater. Res. Soc. Jpn.*, 1994, **16B**, 1053–1056.